**Int. J. Aquat. Biol.** (2025) 13(3): 75-84
ISSN: 2322-5270; P-ISSN: 2383-0956
Journal homepage: www.ij-aquaticbiology.com


Original Article

# Antibacterial activity of green-synthesized gold nanoparticles produced by *Spirulina platensis* algae

**Sara Muonas, Raid Kadhim Abed Alasady***

Department of Biology, College of Education, University of Al-Qadisiyah, Qadisiyah, Iraq.

**Abstract:** Gold nanoparticles (AuNPs) synthesized using green methods are of paramount importance due to their potential in combating antimicrobial resistance and enhancing antioxidant therapies. Incorporating *Spirulina platensis* into nanoparticle synthesis offers a sustainable and eco-friendly alternative that addresses key challenges in modern nanomedicine. This research aimed to evaluate the efficacy of *S. platensis* as a bio-reductant for AuNP synthesis and to assess the resulting nanoparticles' biological activities. The purpose was to establish a reproducible, green synthesis protocol for high-quality AuNPs with improved biomedical potential. *Spirulina platensis* samples were procured in powdered form from a reputable supplier, ensuring consistency and purity for the subsequent extraction and synthesis processes. UV-Visible spectroscopy, XRD, and FE-SEM were used for characterization, while GC-MS analysis indicated bioactive reducing agents in the extract. AuNP production was confirmed by a significant surface plasmon resonance peak at 405 nm in the UV-Visible examination. XRD patterns showed a face-centered cubic structure with a prominent peak at 38° (2θ). The FE-SEM scans showed that the AuNPs were mostly spherical, with an average diameter of 20-30 nm. Antibacterial assays showed inhibition zones of up to 20 mm against *Acinetobacter baumannii* and 18 mm against *Enterococcus faecalis*, with activity being dose-dependent, while antioxidant assays recorded a maximum scavenging inhibition of 73.8% at a concentration of 1 mg/ml. GC-MS analysis identified key bioactive compounds, including fatty acids, which make up approximately 30% of the extract, facilitating effective nanoparticle synthesis. Overall, the study confirms that *S. platensis* is an effective bio-reductant for the green synthesis of gold nanoparticles, which exhibit significant potential for various biomedical applications.

*Article history:*
Received 16 May 2025
Accepted 23 June 2025
Available online 25 June 2025

*Keywords:*
Gold nanoparticles
Green synthesis
Antibacterial activity
Antioxidant assay

## Introduction

The rapid emergence of multidrug-resistant bacterial strains has intensified the search for alternative antimicrobial agents (Banoon et al., 2020; Al-Muhanna et al., 2020; Almutairy, 2024). Among these, gold nanoparticles (AuNPs) have attracted considerable attention due to their unique physicochemical properties and potential biomedical applications. Recent studies have demonstrated that AuNPs synthesized through green methods offer an eco-friendly, cost-effective alternative to conventional chemical routes (Hammami et al., 2021). In this context, the use of marine microalgae such as *Spirulina platensis* has emerged as a promising strategy owing to its rich reservoir of bioactive compounds capable of reducing and stabilizing metal ions during nanoparticle synthesis (Menaa et al., 2021).

AuNPs have garnered significant attention in recent years due to their unique physicochemical properties and potential applications in various fields, including nanomedicine, catalysis, and sensing (Huang et al., 2023). Among the different methods for synthesizing AuNPs, the green synthesis approach, utilizing biological entities such as plants, bacteria, fungi, and algae (Alsaiari et al., 2023). Biological synthesis offers advantages such as cost-effectiveness, reduced toxicity, and the ability to produce stable nanoparticles with controlled sizes and shapes (Ying et al., 2022).

Green synthesis of nanoparticles has emerged as a sustainable alternative to conventional chemical

*Correspondence: Raid Kadhim Abed Alasady
E-mail: raid.al-asady@qu.edu.iq

DOI: https://doi.org/10.22034/ijab.v13i3.2607

methods, offering eco-friendly and cost-effective routes for producing nanomaterials with tailored biological properties (Gupta et al., 2023). Among biological agents, algae have gained prominence due to their rich bioactive compounds, which act as reducing and stabilizing agents during nanoparticle synthesis (Sampath et al., 2022). *Spirulina platensis*, a cyanobacterium, is particularly notable for its high content of proteins, polysaccharides, and antioxidants, making it a promising candidate for the biogenic synthesis of gold nanoparticles (AuNPs) with potential biomedical applications (Al-Badwy et al., 2023). Beyond the synthesis and characterization, the biological activities of these green-synthesized AuNPs are of paramount importance.

Emerging nanobiotechnologies further contextualize the biomedical potential of algal-derived AuNPs. Nanoscale surface engineering of soft materials can precisely tune hydrophilicity, ligand presentation, and cell-material interactions (Kim et al., 2014), complementing the inherent bioactive capping conferred by *Spirulina* metabolites. Parallel antimicrobial platforms, such as biosynthesized chitosan nanoparticles demonstrating broad inhibitory activity (Ali et al., 2022) and reviews highlighting how nanoparticle physicochemistry governs penetration and persistence within protective biofilms (Al-Saady et al., 2022). Beyond direct antibacterial action, iron-oxide nanoparticle-based protein-conjugated nanosystems are advancing as vaccine/adjuvant and drug delivery vehicles (Al-Abboodi et al., 2024; Zainab et al., 2024), suggesting that surface-modifiable gold cores capped with biogenic ligands could be modularly adapted for immunotherapeutic payloads. In addition, microfluidic acoustic and gradient platforms enabling rapid multicellular tumor spheroid formation and chemotaxis modeling (Al-Abboodi et al., 2011; Alhasan et al., 2013; Banoon and Ghasemian, 2022) provide physiologically relevant testbeds where the redox and antimicrobial attributes of *Spirulina*-mediated AuNPs can be probed under 3D tissue-like constraints. Collectively, these strands of literature position the present green synthesis not as an isolated procedural advance but as a foundation for multifunctional nano-assemblies spanning antibiofilm strategies, vaccine delivery, and microphysiological disease modeling.

Therefore, this research aims to evaluate the antibacterial efficacy of *S. platensis*-mediated gold nanoparticles. Furthermore, the antioxidant potential of these nanoparticles will be investigated, as it represents another crucial aspect of their potential biomedical applications. Additionally, the phytochemical composition of *S. platensis* extract, as determined by Gas Chromatography-Mass Spectrometry (GC-MS), will be considered in its role in nanoparticle synthesis and the observed biological activities.

## Materials and Methods

The study was conducted at the Biology Sciences Department laboratories of the College of Education, Al-Qadisiyah University, Iraq, in 2024. Data were collected over several months to ensure robust process optimization and thorough characterization of the synthesized nanoparticles.

**Algal material preparation:** *Spirulina platensis* powder was procured commercially (Amazon Inc., USA) and taxonomically characterized using light microscopy and standard taxonomic keys. The algal powder was stored in airtight containers at 4°C until use (Sudha et al., 2013).

**Preparation of aqueous algal extract:** Aqueous extract was prepared by refluxing 100 g of *S. platensis* powder with 200 mL of deionized water in a Soxhlet apparatus for 3 hours. The extract was filtered through Whatman No. 2 filter paper, concentrated using a rotary evaporator at 40°C, and stored at -20°C for subsequent synthesis (Kalabegishvili et al., 2012).

**Green synthesis of gold nanoparticles (AuNPs):** Gold nanoparticles were synthesized using a one-pot bio-reduction method. Briefly, 800 mL of 1 mM tetrachloroauric acid ($HAuCl_4$) solution was mixed with 200 mL of *S. platensis* aqueous extract under continuous magnetic stirring (25°C, 500 rpm). The color transition from pale yellow to ruby red indicated AuNP formation. The mixture was centrifuged (4,500

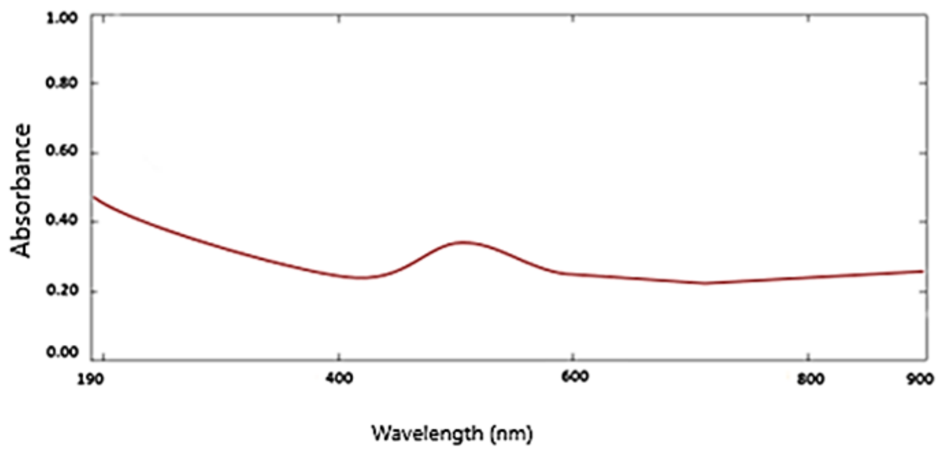


Figure 1. UV-Vis absorption spectrum of AuNPs synthesized using *Spirulina platensis*.

rpm, 30 min), and the pellet was washed twice with deionized water. Purified AuNPs were dried at 50°C and stored as a powder (Veena et al., 2019).

**Characterizations of AuNPs:** The surface plasmon resonance (SPR) of AuNPs was analyzed using a UV-Vis spectrophotometer (190-900 nm range). A distinct peak at ~520 nm confirmed AuNP formation (Huang et al., 2023). Elemental composition was verified using Energy-Dispersive X-ray Spectroscopy (EDX) coupled with FE-SEM (10 kV, 10 mm working distance). Crystallinity was analyzed via X-ray Diffraction (XRD) (Cu-Kα radiation, $\lambda = 1.5406$ Å) over a 2θ range of 10°-80°. Peaks corresponding to (111), (200), (220), and (311) planes confirmed face-centered cubic (FCC) structure (Shi et al., 2012). AuNPs were deposited on silicon substrates and imaged in Atomic Force Microscopy (AFM in tapping mode to evaluate surface topography and particle size (Dhaka et al., 2023).

Functional groups on AuNPs were identified using Fourier Transform Infrared Spectroscopy (FTIR) (500-3,500 $cm^{-1}$ range) to elucidate biomolecules involved in stabilization (Xu et al., 2020). The morphological features of gold nanoparticles (AuNPs) synthesized using *S. platensis* were analyzed using Field-Emission Scanning Electron Microscopy (FE-SEM). A colloidal suspension of AuNPs was prepared by dispersing the nanoparticles in ethanol, followed by sonication for 10 minutes. A drop of the suspension was placed on a silicon stub and air-dried at room temperature. Imaging was performed at accelerating voltages of 5-15 kV and varying magnifications using a MIRA3 TESCAN FE-SEM system. The working distance was maintained at 10 mm to optimize resolution (Mahmoud et al., 2016).

**GC-MS analysis of *S. platensis* extract:** The ethanolic extract was analyzed using an Agilent 7820A GC-MS analysis of *S. platensis* extract system equipped with a HP-5MS column (30 m × 0.25 mm). Helium carrier gas (99.99% purity) was used at 11 psi. Oven temperature was programmed: 80°C (hold 2 min), ramped to 280°C at 8°C/min, then to 300°C at 3°C/min. Bioactive compounds were identified using the NIST library (Deyab et al., 2021).

**Antioxidant activity assay:** The DPPH radical scavenging activity of AuNPs was evaluated. Briefly, 100 µL of AuNPs (0.125-1 mg/mL) was mixed with 100 µL of 0.1 mM DPPH in methanol. After 30 min in darkness, absorbance was measured at 517 nm. Inhibition (%) was calculated according to (Patel et al., 2024), using the equation of Inhibition (%) = $(1 - A_{sample} / A_{control}) \times 100$.

**Antibacterial activity evaluation:** The agar well diffusion method was employed against *Acinetobacter baumannii* and *Enterococcus faecalis*. Bacterial suspensions (0.5 McFarland standard) were swabbed onto Mueller-Hinton agar plates. Wells (8 mm diameter) were loaded with 100 µL of AuNPs (0.5-2 mg/mL). After 24 h incubation at 37°C, inhibition zones were measured (More et al., 2023).

**Statistical Analysis:** Data were expressed as mean ± standard deviation (SD). One-way ANOVA and

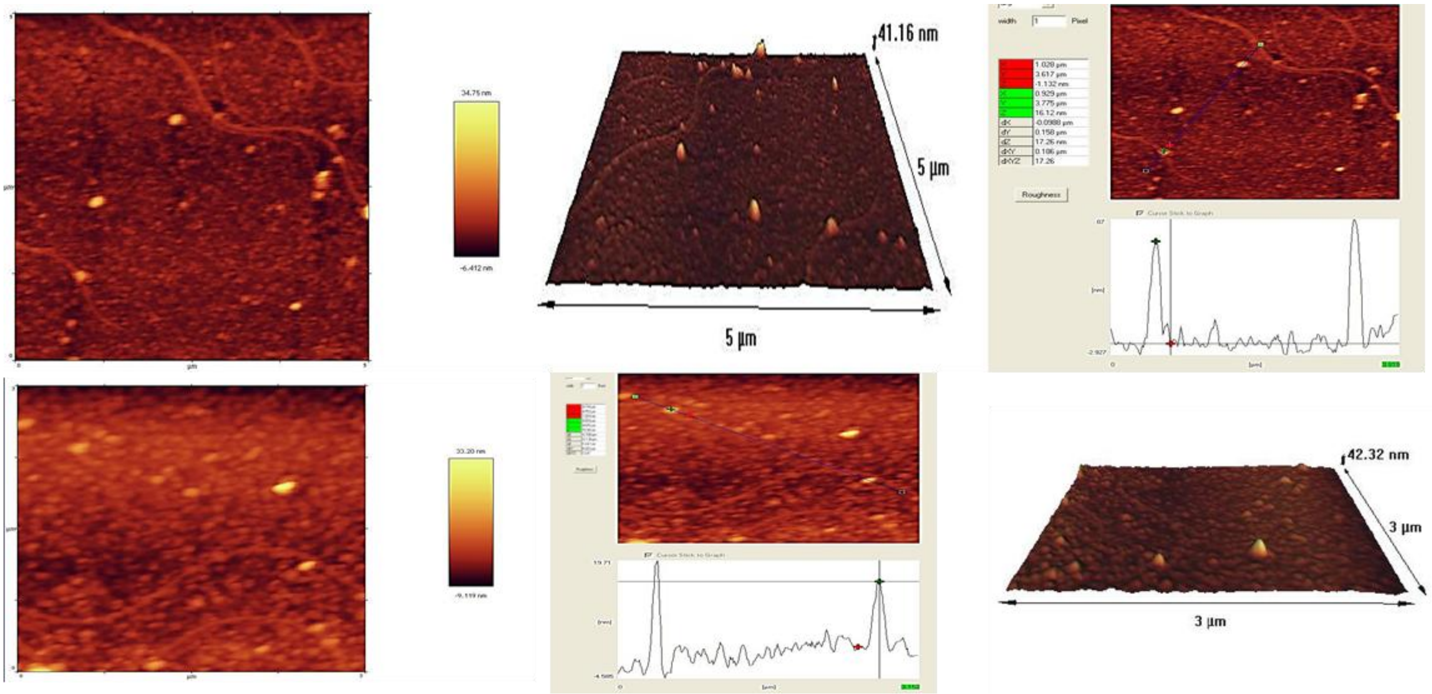


Figure 2. Characterization of gold nanoparticles prepared using *Spirulina platensis* using atomic force microscopy.

Tukey's post-hoc test (SPSS v27) were used for comparisons ($P$<0.05) (Rónavári et al., 2021).

## Results and Discussions

The biosynthesis of gold nanoparticles (AuNPs) using *S. platensis* extract was confirmed by UV-Vis spectroscopy, which exhibited a distinct surface plasmon resonance (SPR) peak at 520 nm (Fig. 1), confirming the successful biosynthesis of AuNPs. SPR arises from the collective oscillation of conduction electrons in metallic nanoparticles when exposed to light, and its position is highly dependent on particle size, shape, and dielectric environment (Huang et al., 2023). The observed peak at 520 nm is characteristic of spherical AuNPs with diameters < 50 nm, consistent with previous reports on algae-mediated synthesis (Díaz-García et al., 2023).

AFM images revealed spherical AuNPs with a homogeneous size distribution of 10-30 nm (Fig. 2). The smooth surfaces and uniform shapes suggested effective stabilization by algal biomolecules. The spherical shape of the AuNPs can be attributed to the isotropic growth facilitated by biomolecules in the algal extract. Proteins, polysaccharides, and phenolic compounds in *S. platensis* likely act as reducing and stabilizing agents, ensuring uniform growth in all directions. This aligns with studies where algal biomolecules guide nucleation and growth phases to produce isotropic nanostructures (Chugh et al., 2021). The narrow size range indicates controlled synthesis conditions. Rapid nucleation followed by regulated growth, mediated by algal metabolites, prevents excessive aggregation. Comparable results were reported by Sudha et al. (2013), where *S. platensis*-derived AuNPs exhibited sizes of 15-35 nm, highlighting the reproducibility of algal-mediated synthesis. The smooth surfaces observed in AFM images suggest effective passivation by algal biomolecules, which form a protective capping layer. This minimizes surface defects and prevents aggregation, critical for stability in biomedical applications. Similar findings were noted in studies using plant extracts, where phytochemicals ensured monodispersity and surface uniformity (Veena et al., 2019).

XRD analysis confirmed the face-centered cubic (FCC) crystalline structure of AuNPs, with characteristic peaks at 38.2°, 44.4°, 64.6°, and 77.5°, corresponding to the (111), (200), (220), and (311) lattice planes, respectively (Fig. 3). The observed peaks correspond to the (111), (200), (220), and (311) lattice planes of FCC gold (JCPDS No. 04-0784),

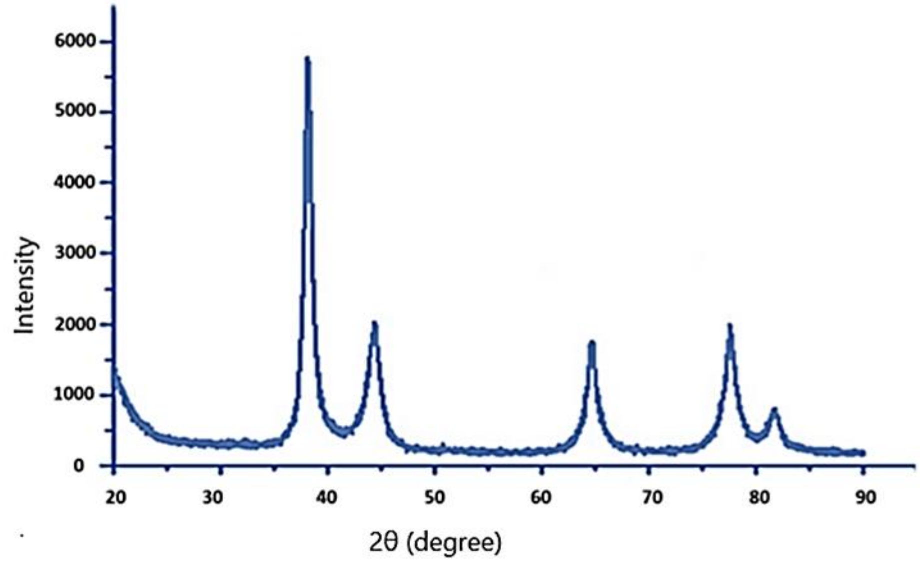


Figure 3. XRD pattern of gold nanoparticles prepared using *Spirulina platensis*.

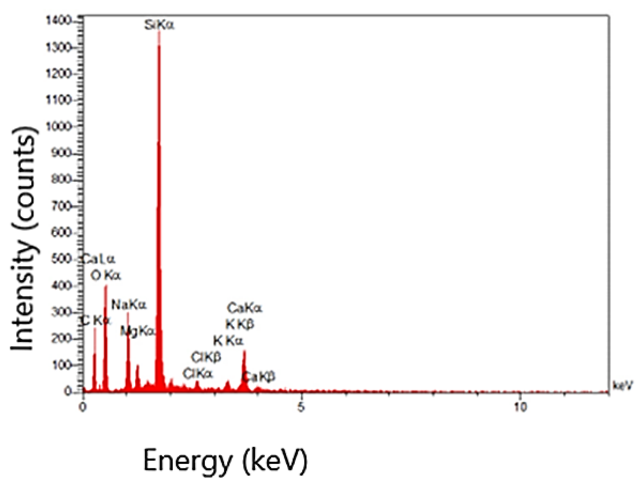


Figure 4. Energy dispersive spectroscopy of gold nanoparticles synthesized using *Spirulina platensis*.

consistent with studies on biogenic AuNPs. Patel et al. (2024) reported similar XRD patterns for AuNPs synthesized using marine algae *Spatoglossum asperum*, attributing the FCC structure to the templating effect of algal polysaccharides. The sharp, well-defined peaks in our study indicate high crystallinity, a hallmark of efficient reduction and stabilization by *S. platensis* biomolecules (Alprol et al., 2023). EDX spectroscopy verified the elemental composition, showing a strong gold signal (~92%) with minor oxygen and carbon peaks, attributed to algal capping agents (Fig. 4).

FTIR analysis identified functional groups such as -OH (3,300 cm$^{-1}$), C=O (1,650 cm$^{-1}$), and N-H (1,540 cm$^{-1}$), indicating the involvement of proteins, polysaccharides, and phenolic compounds in reduction and stabilization (Fig. 5). FE-SEM images (Fig. 6) revealed that *S. platensis*-synthesized AuNPs exhibited spherical morphology with a narrow size distribution of 10-30 nm. The particles displayed smooth surfaces and minimal aggregation, indicative of effective stabilization by algal biomolecules such as polysaccharides and proteins. This aligns with previous studies where AuNPs showed similar monodispersity, attributed to the capping action of phycobiliproteins (El-Sheekh et al., 2023).

AuNPs demonstrated concentration-dependent DPPH radical scavenging activity, with maximum inhibition of 73.79% at 1 mg/mL (Table 1). This efficacy surpasses earlier reports for chemically synthesized AuNPs, likely due to synergistic interactions between the nanoparticle surface and antioxidant phytochemicals (Aldujaili and Banoon 2020; Rosyidah et al., 2024). The scavenging mechanism may involve electron transfer from algal biomolecules to free radicals, stabilizing reactive oxygen species (ROS).

AuNPs exhibited significant antibacterial effects against multidrug-resistant *A. baumannii* and *E. faecalis*, with inhibition zones of 20 and 18 mm, respectively, at 2 mg/mL (Table 2, Fig. 7). The activity was dose-dependent, declining to 11 mm (*A. baumannii*) and 12 mm (*E. faecalis*) at 0.5 mg/ml.

Table 1. Concentration-Dependent antioxidant activity of green-synthesized gold nanoparticles (AuNPs) using Spirulina platensis extract.

| Concentration (mg/ml) | Gold Nanoparticles (Scavenging Inhibition % ± SE) |
|---|---|
| 0.12 | 64.30±0.12[Aa] |
| 0.25 | 69.74±0.08[ABa] |
| 0.5 | 73.65±0.10[Ba] |
| 1 | 73.79±0.18[Ba] |
| Mean±SE | 70.73±2.22[a] |
| LSD at $P$<0.05 | 6.24 |

DPPH Radical Scavenging Inhibition (%) at Different Concentrations (Mean ± Standard Error). Aa, ABa, Ba: Lowercase letters denote significant differences between concentrations (column-wise; $P$<0.05). LSD: Least significant difference at $P$<0.05.

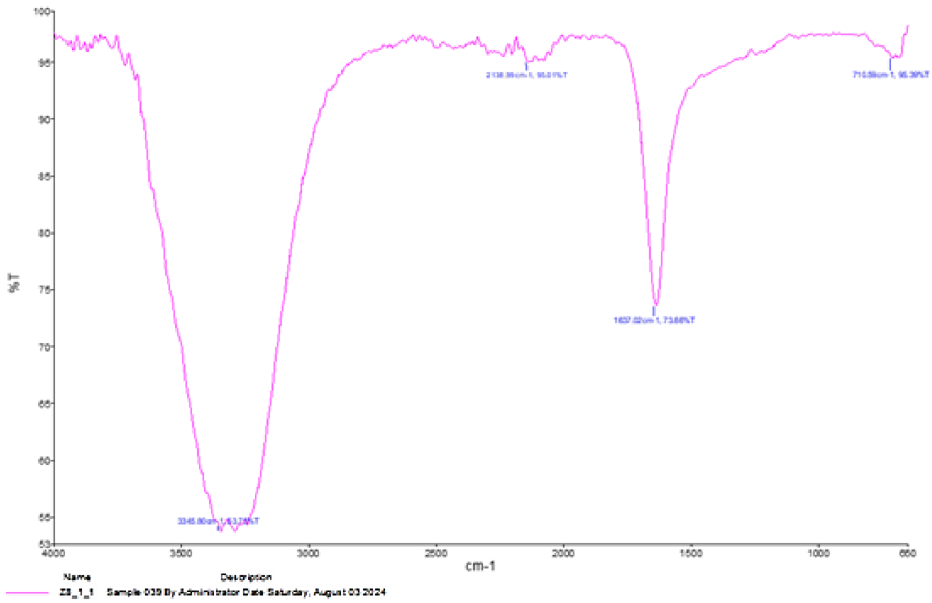


Figure 5. Fourier transform infrared analysis of gold nanoparticles synthesized using *Spirulina platensis*.

These results align with studies highlighting the ability of AuNPs to disrupt bacterial membranes, inhibit ATPase activity, and induce oxidative stress via ROS generation (More et al., 2023). The smaller size and high surface-area-to-volume ratio of AuNPs synthesized here likely enhanced their penetration into bacterial cells (Hassan et al., 2020).

GC-MS analysis of *S. platensis* extract identified hexadecanoic acid methyl ester (34.82%), phytol (10.18%), and neophytadiene (11.66%) as major constituents (Table 3, Fig. 8). These compounds are known for their reducing and stabilizing roles in nanoparticle synthesis. For instance, phytol acts as a surfactant, preventing aggregation, while fatty acids facilitate electron transfer during $Au^{3+}$ reduction (Deyab et al., 2021).

Looking ahead, coupling green-synthesized *Spirulina* AuNP platforms with artificial intelligence (AI) and aquatic informatics could accelerate both rational nanodesign and real-world deployment (Hassan et al., 2023), suggesting that future iterations of this biogenic system could algorithmically tune capping chemistry for targeted antimicrobial or antioxidant performance. Parallel machine-learning frameworks that infer pollution sources in major Iraqi river systems (Rashid et al., 2024) and deep learning pipelines for automated biodiversity surveillance (Salman et al., 2025) illustrate a converging environmental data layer into which stable, low-toxicity AuNP sensors (e.g., functionalized for redox or pathogen markers) could be embedded for continuous eco-health monitoring. As such, sensing networks move toward clinical or public-health interfaces, safeguarding patient and genomic metadata becomes critical; cybersecurity-focused ML filters that flag phishing vectors in healthcare infrastructures

Table 2. AuNPs as antibacterial effects against multidrug-resistant *Acinetobacter baumannii* and *Enterococcus faecalis*.

| Concentration (mg/mL) | *Acinetobacter baumannii* (Mean ± SD) | *Enterococcus faecalis* (Mean±SD) | *P*-value (vs. Control) | Significant? (α=0.05) |
|---|---|---|---|---|
| 0 (Control) | 0.00±0.00 | 0.00±0.00 | - | - |
| 0.5 | 0.00±0.00 | 0.00±0.00 | 1.000 | No |
| 1 | 12.00±0.60 | 12.00±0.90 | < 0.001 | Yes |
| 1.5 | 14.00±0.80 | 16.00±1.10 | < 0.001 | Yes |
| 2 | 20.00±1.20 | 18.00±1.50 | < 0.001 | Yes |

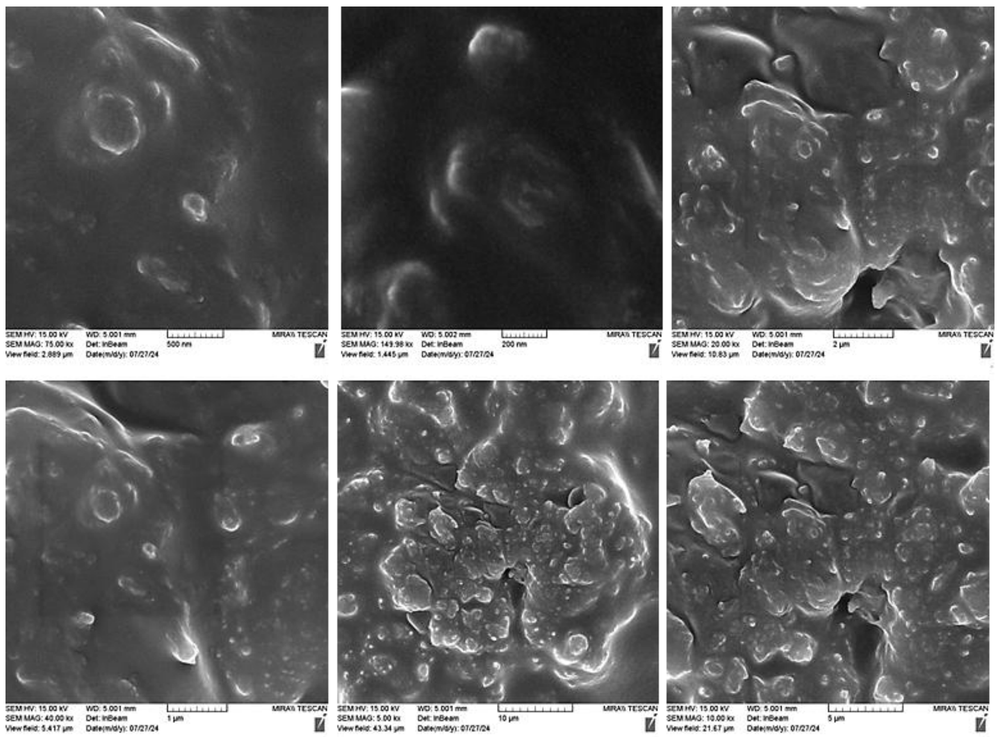

Figure 6. Field-emission scanning electron microscopy (FE-SEM) analysis of green-synthesized gold nanoparticles (AuNPs) using *Spirulina platensis*, revealing spherical morphology and uniform size distribution (10030 nm).


Figure 7. Antibacterial activity (diameter of inhibition zone in mm) of gold nanoparticles (AuNPs) at different concentrations (0.5, 1, 1.5, 2) compared to the control against *Acinetobacter baumannii* (A.B.) and *Enterococcus faecalis* (E.F.) strains.

(Mousa et al., 2025). In parallel, advances in the valorization of naturally occurring minerals—such as the use of diatomaceous earth as a sustainable eco-coagulant for wastewater treatment, optimized via response surface methodology—highlight the broader applicability of green resource utilization strategies in environmental and biomedical nanotechnology contexts (Benouis et al., 2022).

## Conclusion

The feasibility of using *S. platensis* for the green synthesis of gold nanoparticles (AuNPs) has been successfully demonstrated in the present work. The biobased method not only provides an environmentally friendly and cost-effective alternative to conventional chemical synthesis but also produces nanoparticles with desirable optical, structural, and biological properties. The observed

Table 2. AuNPs as antibacterial effects against multidrug-resistant *Acinetobacter baumannii* and *Enterococcus faecalis*.

| Concentration (mg/mL) | *Acinetobacter baumannii* (Mean±SD) | *Enterococcus faecalis* (Mean±SD) | *P*-value (vs. Control) | Significant? (α=0.05) |
|---|---|---|---|---|
| 0 (Control) | 0.00±0.00 | 0.00±0.00 | - | - |
| 0.5 | 0.00±0.00 | 0.00±0.00 | 1.000 | No |
| 1 | 12.00±0.60 | 12.00±0.90 | < 0.001 | Yes |
| 1.5 | 14.00±0.80 | 16.00±1.10 | < 0.001 | Yes |
| 2 | 20.00±1.20 | 18.00±1.50 | < 0.001 | Yes |

Table 3. Analysis of chemical compounds extracted from *Spirulina platensis* using Gas Chromatography-Mass Spectrometry (GC-MS)

| No | RT (min) | Area% | Name | Quality |
|---|---|---|---|---|
| 1 | 22.221 | 1.78 | 2,4-Dihydroxybenzoic acid, 3TMS derivative | 35 |
| 2 | 22.351 | 6.19 | Heptadecane | 99 |
| 3 | 24.722 | 11.66 | Neophytadiene | 97 |
| 4 | 24.888 | 1.28 | 2-Hexadecene, 3,7,11,15-tetramethyl-, [R-[R*, R*-(E)]]- | 83 |
| 5 | 25.122 | 2.06 | 1-Methoxy-3-(2-hydroxyethyl) nonane | 58 |
| 6 | 25.423 | 3.21 | Neophytadiene | 53 |
| 7 | 25.547 | 2.68 | Methyl hexadec-9-enoate | 96 |
| 8 | 25.941 | 34.82 | Hexadecanoic acid, methyl ester | 99 |
| 9 | 28.214 | 8.68 | 6,9,12-Octadecatrienoic acid, methyl ester | 98 |
| 10 | 28.494 | 11.44 | 9,15-Octadecadienoic acid, methyl ester, (Z, Z)- | 99 |
| 11 | 28.915 | 10.18 | Phytol | 91 |
| 12 | 31.348 | 2.58 | Palmitoyl chloride | 30 |
| 13 | 40.843 | 3.45 | Cyclotrisiloxane, hexamethyl- | 50 |

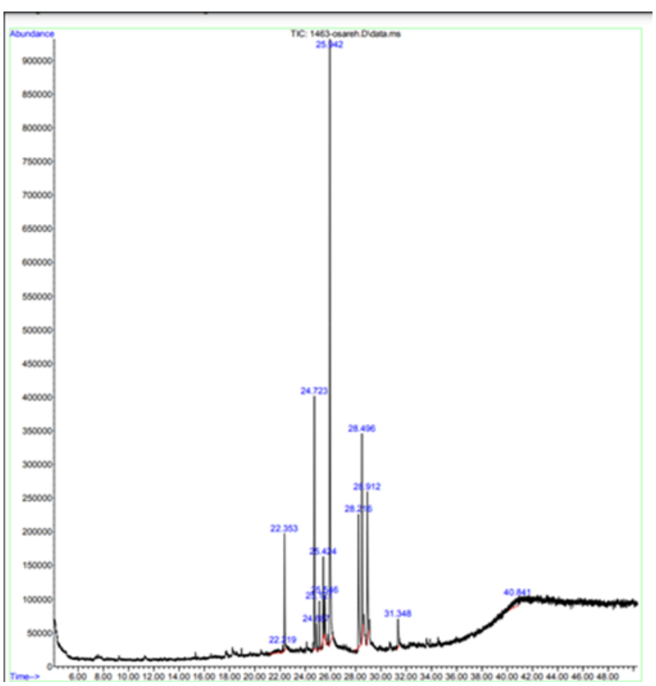


Figure 8. Gas Chromatography-Mass Spectrometry (GC-MS) analysis of the chemical compounds of the second algae.

surface plasmon resonance (SPR) peak between 390 and 420 nm confirms the formation of spherical and evenly distributed gold nanoparticles. X-ray diffraction (XRD) analysis further confirmed the crystalline nature of the synthesized gold nanoparticles, indicating a well-defined face-centered cubic (FCC) structure. Morphological examinations using FE-SEM and elemental verification by EDX confirmed the purity and homogeneity of the nanoparticles, demonstrating the effectiveness of *S. platensis* as a reducing and stabilizing agent. GC-MS analysis of the *Spirulina* extract provided insights into the group of secondary metabolites responsible for the reduction of gold ions and subsequent stabilization of the nanoparticles. The presence of fatty acids and phenolic compounds appears to play a crucial role in ensuring the high quality and stability of the gold nanoparticles. Furthermore, biological evaluations—including antibacterial, antioxidant, and antihemolytic activities—showed that these biosynthesized nanoparticles hold great potential for biomedical applications. They exhibited potent antibacterial activity against common pathogens, along with a dose-dependent antioxidant effect, supporting their utility in future therapeutic strategies.

## References


Al-Abboodi A., Albukhaty S., Sulaiman G.M., Al-Saady M.A., Jabir M.S., Abomughaid M.M. (2024). Protein conjugated superparamagnetic iron oxide nanoparticles for efficient vaccine delivery systems. Plasmonics, 19(1): 379-388.

Al-Abboodi A., Tjeung R., Doran P., Yeo L., Friend J., Chan P. (2011). Microfluidic chip containing porous gradient for chemotaxis study. Smart Nano-Micro Materials and Devices, 8204: 219-224.

Al-Badwy\ A.H., Khalil A.M., Bashal A.H., Kebeish R. (2023). Polysaccharides from *Spirulina platensis* (PSP): promising biostimulants for the green synthesis of silver nanoparticles and their potential application in the treatment of cancer tumors. Microbial Cell Factories, 22 (1): 247.

Aldujaili N.H., Banoon S.R. (2020). Antibacterial characterization of titanium nanoparticles nanosynthesized by *streptococcus thermophilus*. Periódico Tchê Química, 17(34): 311-320.

AlHasan L., Qi A., Al-Abboodi A., Rezk A., Shilton R.R., Chan P.P., ... Yeo L. (2013). Surface acoustic streaming in microfluidic system for rapid multicellular tumor spheroids generation. Micro/Nano Materials, Devices, and Systems, 8923: 828-831

Ali Z.H., Al-Saady M.A.A.J., Aldujaili N.H., Rabeea Banoon S., Abboodi A. (2022). Evaluation of the antibacterial inhibitory activity of chitosan nanoparticles biosynthesized by *Streptococcus thermophilus*. Journal of Nanostructures, 12(3): 675-685.

Al-Muhanna S.G., Banoon S.R., Al-Kraety I.A.A. (2020). Molecular detection of integron class 1 gene in proteus mirabilis isolated from diabetic foot infections. Plant Arch, 2(1): 3101-7.

Almutairy B. (2024). Extensively and multidrug-resistant bacterial strains: case studies of antibiotics resistance. Frontiers in Microbiology, 15: 1381511.

Alprol A.E., Mansour A.T., Abdelwahab A.M., Ashour M. (2023). Advances in green synthesis of metal oxide nanoparticles by marine algae for wastewater treatment by adsorption and photocatalysis techniques. Catalysts, 13(5): 888.

Al-Saady A.J., Aldujaili N.H., Banoon S.R., Al-Abboodi A. (2006). Antimicrobial properties of nanoparticles in biofilms. Revis Bionatura, 7(4): 71.

Alsaiari N.S., Alzahrani F.M., Amari A., Osman H., Harharah H.N., Elboughdiri N., Tahoon M.A. (2023). Plant and microbial approaches as green methods for the synthesis of nanomaterials: Synthesis, applications, and future perspectives. Molecules (Basel, Switzerland), 28(1): 463.

Banoon S., Ali Z., Salih T. (2020). Antibiotic resistance profile of local thermophilic Bacillus licheniformis isolated from Maysan province soil. Comunicata Scientiae, 11: e3291-e3291.

Banoon S.R., Ghasemian A. (2022). The characters of graphene oxide nanoparticles and doxorubicin against HCT-116 colorectal cancer cells in vitro. Journal of Gastrointestinal Cancer, 53(2): 410-414.

Chugh D., Viswamalya V.S., Das B. (2021). Green synthesis of silver nanoparticles with algae and the importance of capping agents in the process. Journal, Genetic Engineering and Biotechnology, 19(1): 126.

Benouis K., Khane Y., Ahmed T., Albukhaty S., Banoon S.R. (2022). Valorization of diatomaceous earth as a sustainable eco-coagulant for wastewater treatment: optimization by response surface methodology. Egyptian Journal of Chemistry, 65(9): 777-788.

Deyab M., El-Sheekh M., Hasan R., Elsadany A., Abu Ahmed S. (2021). Phytochemical components of two cyanobacterial local strains. Scientific Journal for Damietta Faculty of Science, 11(1): 67-75.

Dhaka A., Chand Mali S., Sharma S., Trivedi R. (2023). A review on biological synthesis of silver nanoparticles and their potential applications. Results in Chemistry, 6: 101108.

Díaz-García V., Haensgen A., Inostroza L., Contreras-Trigo B., Oyarzun P. (2023). Novel microsynthesis of high-yield gold nanoparticles to accelerate research in biosensing and other bioapplications. Biosensors, 13(12): 992.

Gupta D., Boora A., Thakur A., Gupta T.K. (2023). Green and sustainable synthesis of nanomaterials: Recent advancements and limitations. Environmental Research, 231(3):116316.

Hammami I., Alabdallah N.M., Jomaa A.A., Kamoun M. (2021). Gold nanoparticles: Synthesis properties and applications. Journal of King Saud University, Science, 33(7): 101560.

Hassan B.A., Lawi, Z.K.K., Banoon S.R. (2020). Detecting the activity of silver nanoparticles, *pseudomonas* *fluorescens* and *Bacillus circulans* on inhibition of *Aspergillus niger* growth isolated from moldy orange fruits. Periódico Tchê Química, 17(35): 678-690.

Hassan S.A.D.H., Almaliki M.N.S., Hussein Z.A., Albehadili H.M., Rabeea Banoon S., Abboodi A., Al-Saady M. (2023). Development of nanotechnology by artificial intelligence: A comprehensive review. Journal of Nanostructures, 13(4): 915-932.

Huang H., Liu R., Yang J., Dai J., Fan S., Pi J., Wei Y., Guo X. (2023). Gold nanoparticles: Construction for drug delivery and application in cancer immunotherapy. Pharmaceutics, 15(7): 10383270.

Kalabegishvili T., Kirkesali E., Rcheulishvili A. (2012). Synthesis of gold nanoparticles by blue-green algae *Spirulina platensis*. 14 p. Retrieved from: https://inis.iaea.org/search/search.aspx?orig_q=RN:43108872

Kim Y., Abuelfilat A.Y., Hoo S.P., Al-Abboodi A., Liu B., Ng T., ... Fu J. (2014). Tuning the surface properties of hydrogel at the nanoscale with focused ion irradiation. Soft Matter, 10(42): 8448-8456.

Mahmoud W.M., Abdelmoneim T.S., Elazzazy A.M. (2016). The impact of silver nanoparticles produced by *Bacillus pumilus* as antimicrobial and nematicide. Frontiers in Microbiology, 7: 1746.

Menaa F., Wijesinghe U., Thiripuranathar G., Althobaiti N.A., Albalawi A.E., Khan B.A., Menaa B. (2021). Marine algae-derived bioactive compounds: A new wave of nanodrugs? Marine Drugs, 19(9): 484.

More P.R., Pandit S., Filippis A.D., Franci G., Mijakovic I., Galdiero M. (2023). Silver nanoparticles: Bactericidal and mechanistic approach against drug resistant pathogens. Microorganisms, 11(2): 9961011.

Mousa A.A., Hassan S.A.D.H., Rashid M.K., Al-Saady M. (2025). Safeguarding Patient Data: Machine Learning for Phishing URL Detection in Healthcare Systems. Journal of Advanced Research Design, 131(1): 47-60.

Patel D., Patel B., Yadav V.K., Sudhakar M.P., Alharbi S.A., Salmen S.H., Patel I., Choudhary N., Patel A. (2024). Silver nanoparticles synthesized from marine algae *Spatoglossum asperum*: Antioxidant properties and seed germination enhancement. Journal of Hazardous Materials Advances, 16: 100478.

Rashid M.K., Salman I.R., Obaid A.L., Hassan S.A.D.H., Al-Musawi M.R., Al-Saady M. (2024). Application of machine learning in predicting sources of water pollution in the Euphrates and Tigris rivers in Iraq. International Journal of Aquatic Biology, 12(6): 581-589.

Rónavári A., Igaz N., Adamecz D.I., Szerencsés B., Molnar C., Kónya Z., Pfeiffer I., Kiricsi M. (2021). Green silver and gold nanoparticles: Biological synthesis approaches and potentials for biomedical applications. Molecules (Basel, Switzerland), 26 (4): 844.

Salman I.R., Rasheed A.A., Hassan S.A.D.H., Hussein R.A., Al-Saady M. (2025). Automated aquatic biodiversity monitoring using deep learning on the Tigris River: Species identification and ecosystem assessment. International Journal of Aquatic Biology, 13(1): 30-40.

Sampath S., Madhavan Y., Muralidharan M., Sunderam V., Lawrance A.V., Muthupandian S. (2022). A review on algal mediated synthesis of metal and metal oxide nanoparticles and their emerging biomedical potential. Journal of Biotechnology, 360: 92-109.

Shi W., Casas J., Venkataramasubramani M., Tang L. (2012). Synthesis and characterization of gold nanoparticles with plasmon absorbance wavelength tunable from visible to near infrared region. ISRN Nanomaterials, 2012: 1-9.

Sudha S.S., Rajamanickam K., Rengaramanujam J. (2013). Microalgae mediated synthesis of silver nanoparticles and their antibacterial activity against pathogenic bacteria. Indian Journal of Experimental Biology, 51(5): 393-399.

Veena S., Devasena T., Sathak S.S.M., Yasasve M., Vishal L.A. (2019). Green synthesis of gold nanoparticles from *Vitex negundo* leaf extract: Characterization and in vitro evaluation of antioxidant–antibacterial activity. Journal of Cluster Science, 30(6): 1591-1597.

Xu L., Wang Y.-Y., Huang J., Chen C.-Y., Wang Z.-X., Xie H. (2020). Silver nanoparticles: Synthesis, medical applications and biosafety. Theranostics, 10(20): 8996-9031.

Ying S., Guan Z., Ofoegbu P.C., Clubb P., Rico C., He F., Hong J. (2022). Green synthesis of nanoparticles: Current developments and limitations. Environmental Technology and Innovation, 26: 102336.

Zainab J.M., Sahira K., Al-Abboodi A.K., Alsaady H.A. (2024). Enhancing pediculicidal activity against *Pediculus humanus capitis* using iron oxide nanoparticle-based formulations of some plant extracts and acetic acid solution. Nigerian Journal of Parasitology, 45(2).